Nano Energy 59 (2019) 434–442

Contents lists available at ScienceDirect

Nano Energy

journal homepage: www.elsevier.com/locate/nanoen

Full paper

# Multifunctional triboelectric nanogenerator towards impact energy harvesting and safeguards

Sheng Wang, Li Ding, Yu Wang*, Xinglong Gong*

*CAS Key Laboratory of Mechanical Behavior and Design of Materials, Department of Modern Mechanics, CAS Center for Excellence in Complex System Mechanics, University of Science and Technology of China (USTC), Hefei 230027, PR China*

ARTICLE INFO

*Keywords:*
Triboelectric nanogenerator
Impact energy
Shear stiffening gel
Polytetrafluoroethylene
Safeguarding property

ABSTRACT

The widespread impact kinetic energy always causes injury and property loss in daily life. Conventional safeguarding systems protect human beings by passively insulating and dissipating impact energy but have ignoring exploring them. Triboelectric nanogenerator (TENG) proves to be a favorable device in harvesting mechanical energy but shows no protection property. Thus, developing novel safeguarding material with energy-harvesting performance is essential in future generation personal security field. Here, a multifunctional TENG capable of collecting impact kinetic energy with safeguarding property is reported by assembling Al foil with hybrid polymer matrix. The matrix is fabricated by incorporating polytetrafluoroethylene (PTFE) nano-particles into shear stiffening (SST) gel and polydimethylsiloxane (PDMS). The optimized TENG (6 mm) after introducing 1% PTFE nano-fillers into hybrid polymer attains the maximum electrical voltage, current and output power of 44.20 V, 8.84 μA and 390.73 μW, respectively. More importantly, SST/PDMS/PTFE-based TENG generates an instantaneous power density of 135.57 $\mu W/m^2$ under low velocity impact. The impact force simultaneously decreases from 1971.90 to 839.72 N, exhibiting a remarkable safeguarding property. Finally, a wearable TENG-based electronic skin can capture external impact energy into electrical energy, resist the impact and precisely map force distribution which demonstrates promising application in next generation smart wearable systems.

## 1. Introduction

Impact with various speeds often occurs in daily life from sport, car accident, ocean waves and even ballistic shooting. The excessive impact kinetic energy during these collisions may cause discomfort, injury, property loss and even death. It is reported approximate 50 million traffic-related injuries and 1.2 million fatalities occur every year worldwide [1]. Therefore, it is still urgent to develop functional safeguarding technologies with monitoring and dissipating impact excitations due to the increasing public concern regarding the disadvantageous influence of harsh collision [2–6]. For example, helmet effectively resisted impact, decreased the force and provided safeguards for passengers [7]. The graphene-coated polymer foam nanocomposite could resist impact pressure and transform it into electrical signals which could act as impact sensor [5]. A structural wood material showed a more than tenfold increment in strength and toughness than natural wood which exhibited excellent ballistic energy absorption performance for body armors [8].

Recently, various novel smart materials also have been developed to meet the rapid development of safeguards [9]. One kind of smart material is shear stiffening composites which include liquid shear thickening fluid and solid shear stiffening (SST) polymer [10]. As a derivative of polyborondimethylsiloxane (PBDMS), SST enables to change from viscous state to rigidity under impact. Thus, SST shows promising applications in shock absorber and safeguards because of its stability, without sealing and controllable mechanical properties [11,12]. A magnetic SST-based smart polymer composite could change the storage modulus from $10^2$ to $10^6$ Pa which demonstrated excellent shear stiffening effect [13]. The maximum energy dissipation of Kevlar/SST/Kevlar sandwich was 20.8 J which presented 60% anti-impact increment than neat Kevlar fiber [14]. So far, most reported systems passively protected human beings by dissipating impact energy but have ignored exploiting them. Therefore, it is still an important issue to develop smart safeguarding devices with the property of detecting and converting impact energy.

Since first reported in 2012, triboelectric nanogenerator (TENG) proves to be a promising renewable energy conversion device owing to the triboelectric effect [15,16]. The triboelectric charges always aggregate in the process of contact-separation and thus, a voltage difference occurs on the surface of the two materials [17–20]. So far, the

* Corresponding authors.
*E-mail addresses:* wyu@ustc.edu.cn (Y. Wang), gongxl@ustc.edu.cn (X. Gong).

https://doi.org/10.1016/j.nanoen.2019.02.060
Received 24 December 2018; Received in revised form 13 February 2019; Accepted 22 February 2019
Available online 26 February 2019

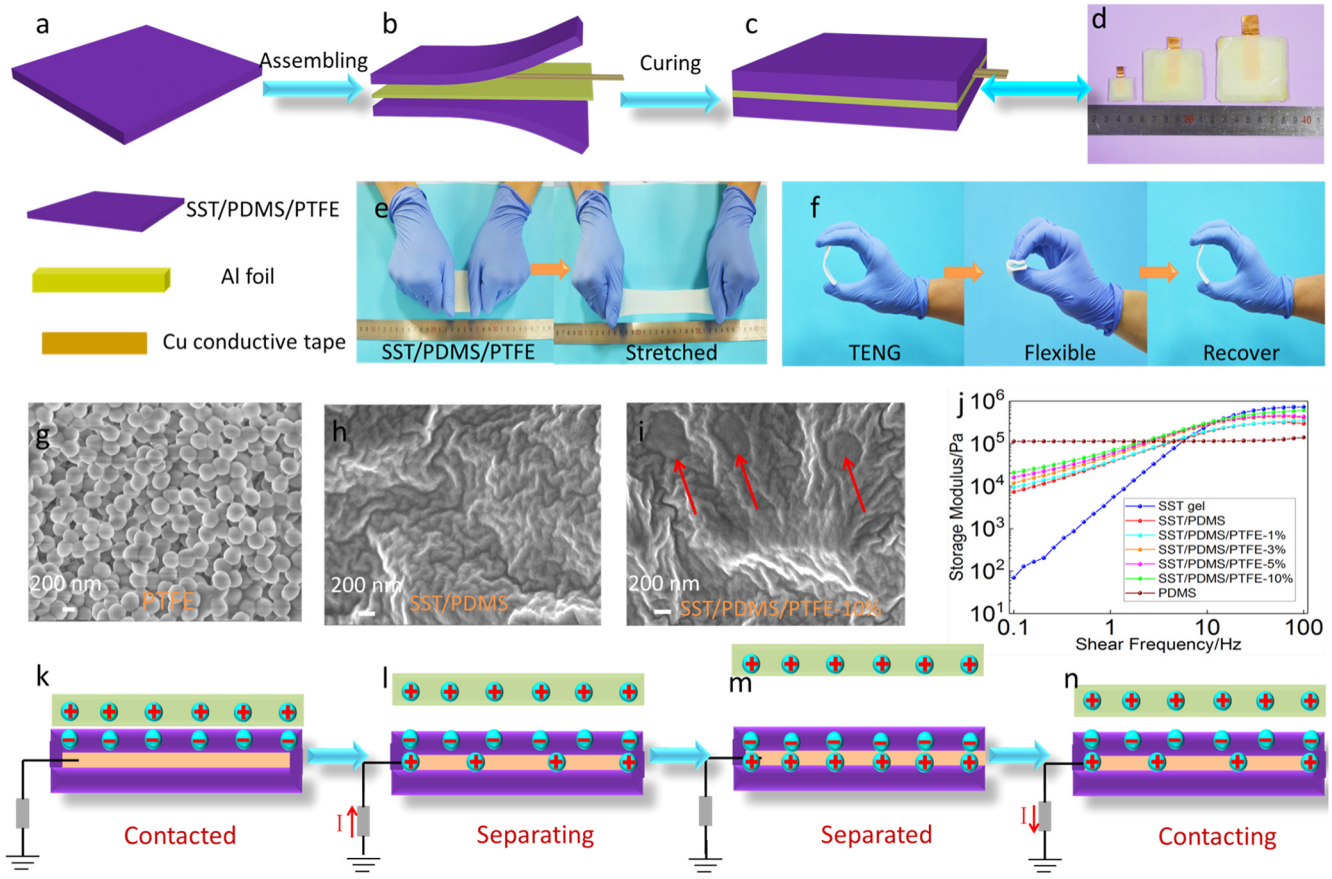


**Fig. 1.** The preparation procedures of TENG: (a) SST/PDMS/PTFE hybrid polymer matrix, (b) assembling and (c) curing TENGs; (d) the as-prepared TENGs with different shapes; (e) stretchability of SST/PDMS/PTFE; (f) flexibility of TENG; SEM images of: (g) PTFE nano-particles, (h) SST/PDMS and (i) SST/PDMS/PTFE-10%; (j) shear stiffening effect of polymer composites; (k–n) working mechanism of the TENG.

developed TENG could harness various frequencies of irregular mechanical energy into electrical energy [21–25]. Additionally, various TENGs with other functions have also been developed to meet the demand of practical applications, such as catalysis [26,27], breath sensing [28] and sterilization [29]. Nowadays, novel TENGs capable of collecting impact energy are proposed and these systems could also act as self-powered sensors to detect external stimulations. A new self-powered TENG could drive itself by gathering fall impact energy into electric energy and as a force sensor, it could detect the falling force of older people which showed promising application in smart hospitals [30]. Apart from sensing dynamic force, a multifunctional single-electrode TENG device could also inhibit the growth of bacterial [31]. A TENG-based acceleration sensor exhibited a high impact sensing range over 18,000 g and a thickness-dependent sensitivity theoretical model was also explored [32]. Although these functional TENG devices present the ability of harnessing impact energy and other functions, they still lack the properties of protecting human beings from harsh injure. Combining shear stiffening polymer with TENG may endow it with the capacity of harvesting impact kinetic energy as well as protecting human beings. Thus, with the rise of personal security awareness nowadays, it will be an exciting work to develop SST-based TENG for its fundamental significance and practical applications.

In this work, a multifunctional TENG with energy-harvesting and safeguarding performance is fabricated with a hybrid polymer matrix and Al foil. The hybrid shear stiffening polymer/polydimethylsiloxane/polytetrafluoroethylene (SST/PDMS/PTFE) composite shows typical shear stiffening effect which the storage modulus (G′) increase from 7.36 kPa to 0.30 MPa in the shear frequency range of 0.1–100 Hz. The PTFE contents and thickness dependent electric properties of TENG are also systematically explored. SST/PDMS/PTFE-1%-based TENG with 6 mm shows 44.20 V and power of 390.73 μW, demonstrating ideal high-frequency energy-collecting property. Moreover, drop hammer test systems are applied to study the safeguarding and energy-gathering performance under low velocity collision conditions. SST/PDMS/PTFE-1%-based TENG (6 mm) produces an output voltage and a maximum power density of 34.93 V and 135.57 $\mu W/m^2$ as well as decreases the impact force by 57.41% which provides protection performance. Finally, a wearable TENG array can collect kinetic energy and resist external impact effectively.

## 2. Experimental sections

### 2.1. Preparation of TENG

SST gel was prepared by heating dimethyl silicone oil with small amount of pyroboric acid for several hours [12] and the solid SST polymer could be obtained after cooling down the reactants. Then, SST gel and HTV silicone rubber (MVQ 110-2, purchased from Dong Jue Fine Chemical Nanjing Co., Ltd) with the ratio of 7: 3 were mixed by a two-roll miller followed by introducing benzoyl peroxide and PTFE nano-particles. After curing the above composites at 100 ℃ under 20 MPa by a plate vulcanizer (Bought from Shanghai Yeshuai Precision Technology. Co. Ltd, YS20T-S), the hybrid polymer matrix could be prepared.

The above hybrid polymer composites were assembled with Al foil, Cu conductive adhesive tape and then placed on steel mould and heated at 80 ℃ under 20 MPa for several minutes. By changing the shapes of moulds, various sizes of TENGs could be fabricated.

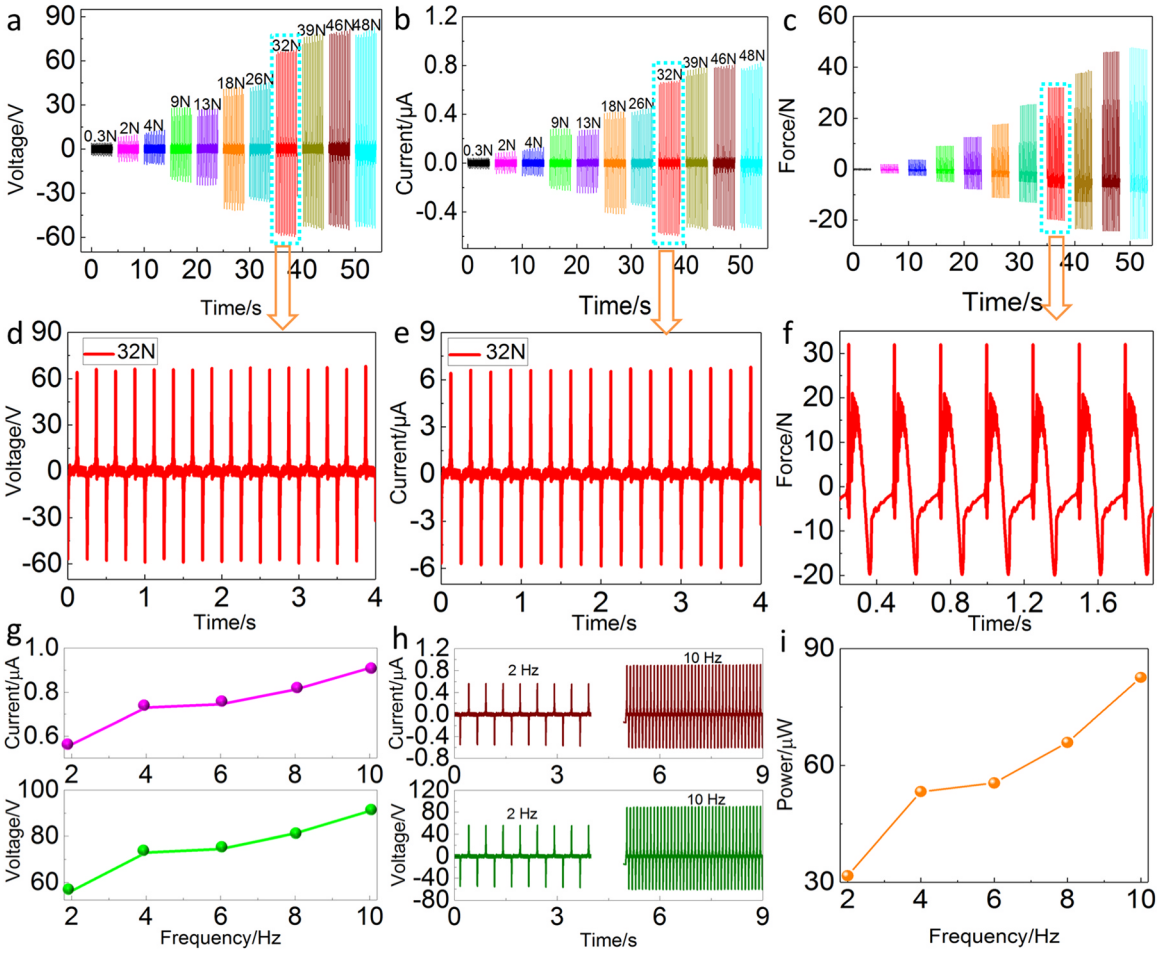


**Fig. 2.** Characterization of TENGs. (c) The loading force dependent (a) voltage and (b) current of SST/PDMS-based TENG at the frequency of 4 Hz; (d) typical voltage and current of TENG under the force of (f) 32 N with external resistance of 100 MΩ; (g) the compression frequency dependence of current-voltage and (i) power at the force of 32 N; (h) the stability of current and voltage of TENG under the excitation of 2 and 10 Hz.

### 2.2. Characterization systems

The mirco-structures of PTFE nano-particles and TENG were characterized by SEM (Gemini SEM 500, ZEISS). Rheological properties of the polymer matrix were measured by a commercial rheometer (Physica MCR 301, Anton Paar Co., Austria). The tested samples were fixed into cylinder with diameter of 10 mm and thickness of 1 mm. The shear frequency varied from 0.1 Hz to 100 Hz. The triboelectric tests were conducted by an oscillator (JZK-10) (bought from Sinocera. Piezotronics. INC, China) and the corresponding output signals were recorded by digital multi-meters (DMM6001). The energy-collecting and safeguarding properties of TENG device was explored by a drop hammer test systems.

## 3. Results and discussion

### 3.1. Characterization of SST/PDMS-based TENG

Fig. 1a–c is the description of the preparation procedures of TENG. Briefly, PTFE nano-particles and small amount of PDMS are introduced into SST polymer by a two-roller miller. Then, the TENG device is fabricated by sealing Al foil with a hybrid SST/PDMS/PFTE polymer matrix and different shapes of TENGs are shown in Fig. 1d. Originated from shear stiffening gel, the hybrid SST/PDMS/PTFE shows stretchable characteristic (Fig. 1e). Additionally, the as-prepared TENG can be bent and totally recovered back (Fig. 1f). The micro-structures of the composites are also characterized. PTFE nano-fillers are spherical particles with a uniform diameter of about 270 nm (Fig. 1g). Many wrinkles can be observed on the surface of SST/PDMS (Fig. 1h), indicating its soft characteristic. Larger PTFE nano-particles appear on the surface of SST/PDMS/PTFE-10% which is due to the agglomeration of PTFE in the mixing process (Fig. 1i).

Shear stiffening gel is a plastic polymer which can be molded into different shapes [13]. However, it turns to stiff under impact. Therefore, its initial storage modulus (G′) is as low as 69.91 Pa under 0.1 Hz shear excitation while its maximum G′ can reach 0.73 MPa (at 100 Hz) which shows typical shear stiffening effect (Fig. 1j). The G′ of PDMS is independent of shear frequency which is about 0.11 MPa. Undoubtedly, the initial G′ of SST/PDMS is increased to 7.36 kPa due to the introduction of PDMS and its maximum G′ is 0.30 MPa which also exhibits shear rate-dependent property. However, the initial modulus of SST/PDMS/PTFE continues increasing due to the enhancement of nano-fillers. To this end, SST/PDMS and SST/PDMS/PTFE are ideal polymer matrixes for flexible electronics.

The working mechanism for harvesting energy of TENG in one cycle process is presented in Fig. 1k–n. Based on the coupling effect of triboelectrification and electrostatic induction [33], the initial contact induces charge transfer at the interface of human skin and TENG owing to their different electron affinity [34,35]. It generates negative triboelectric charges on TENG and positive ones on human skin. After the positive skin finger leaves, a potential difference between Al foil embedded in SST/PDMS/PTFE and the ground is generated and thus results in the flow of free electrons (Fig. 1k, l). The system turns to electrostatic equilibrium when human skin leaves far away (Fig. 1m).

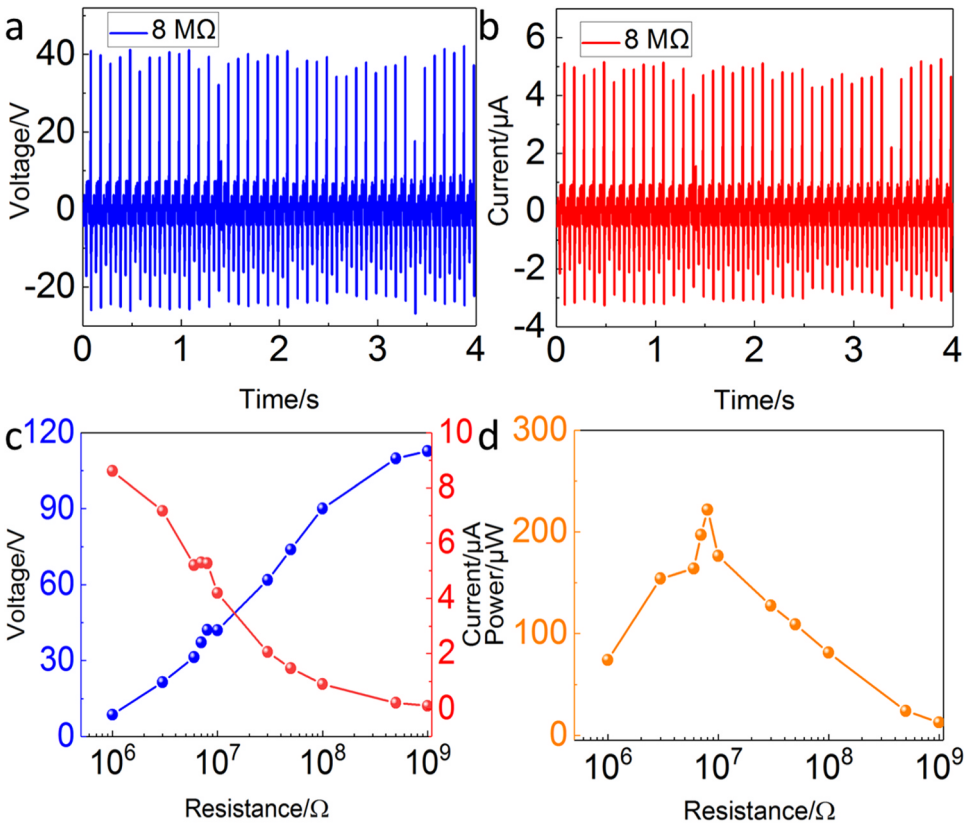


**Fig. 3.** Typical curves of (a) voltage and (b) current of SST/PDMS-based TENG (2 mm) on 8 MΩ load resistance at the force and frequency of 32 N and 10 Hz, respectively. (c) Voltage, current and (d) output powers under various external resistance.

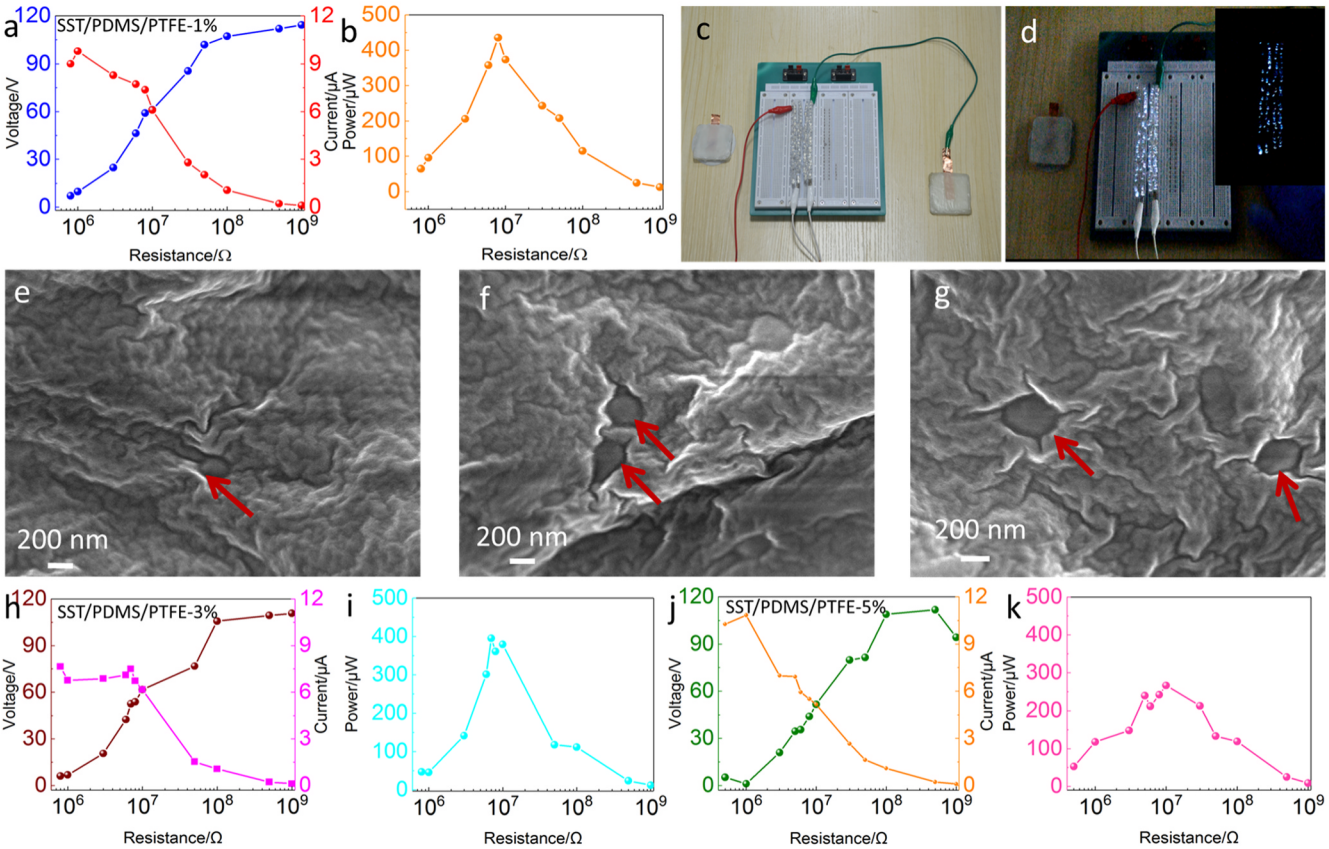


**Fig. 4.** PTFE contents dependent triboelectric performance of TENGs. (a) Voltage, current and (b) power of SST/PDMS/PTFE-1%-based TENG under different external resistance; (c, d) photos of 80 LEDs are brightly lit up by gentle hand tapping on TENG; SEM images of (e) SST/PDMS/PTFE-1%, (f) SST/PDMS/PTFE-3%, (g) SST/PDMS/PTFE-5%; (h, j) electric output including voltage, current and (i, k) power of SST/PDMS/PTFE as a function of PTFE content ranging from 3% to 5% with various external resistance.

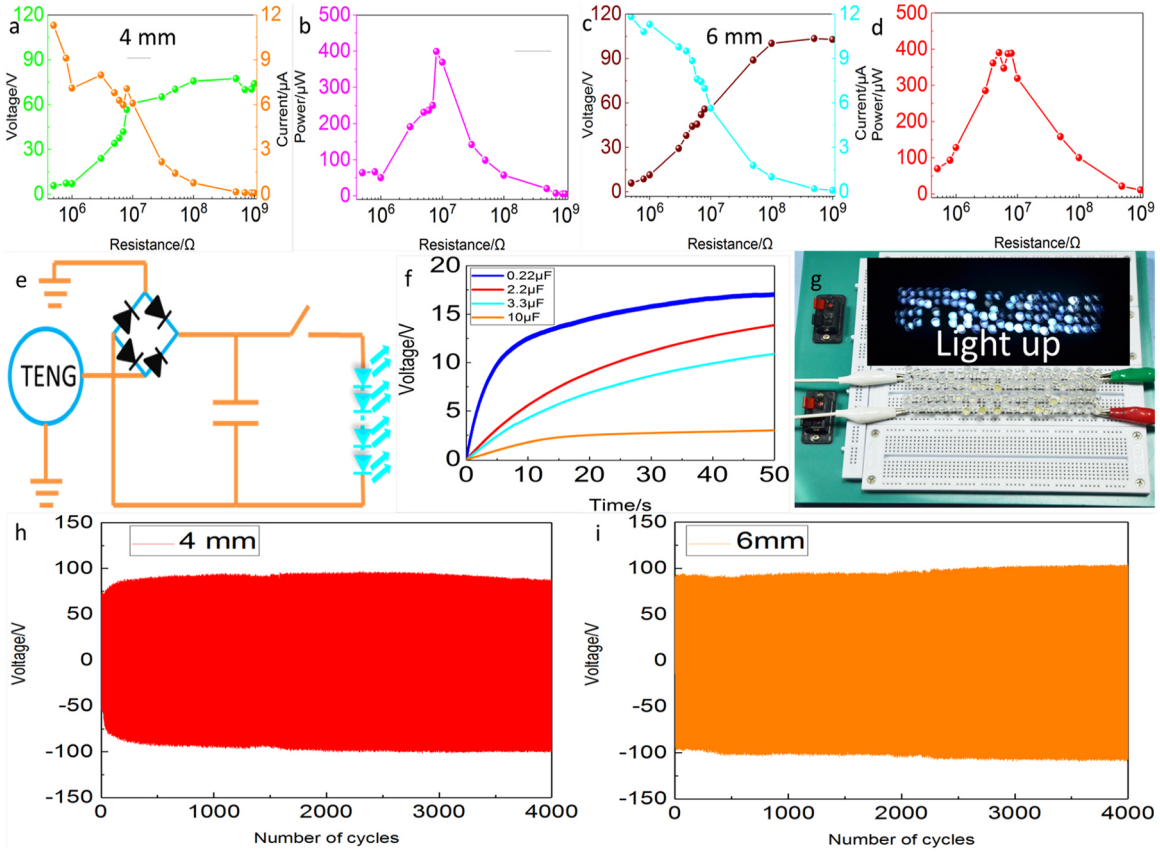


**Fig. 5.** Energy-harvesting properties of SST/PDMS/PTFE-1%-based TENGs with different thicknesses. Voltage, current and the corresponding power as a function of load resistance: (a, b) 4 mm, (c, d) 6 mm; (e) the equivalent circuit for TENG, charging capacitors, rectifier and LED arrays, (f) charging curves by TENG (6 mm) at different load capacitances, (g) images of over 80 LEDs are lit up by the charged capacitor, cyclic stability of TENG with thickness of (h) 4 and (i) 6 mm.

Once human finger is approaching to SST/PDMS/PTFE again, the increased potential in Al foil can drive the free electrons to flow back from the ground which generates a negative current signal until the system reverses to the initial state (Fig. 1n). Thus, the as-prepared TENG can sustainably harvest kinetic energy with cyclic contacting-separating processes and TENG enables to act as a sustainable power source for wearable electronics.

The vertical force and frequency dependent output electrical performance of SST/PDMS-based TENG with sizes of 50 × 50 × 2 $mm^3$ were systematically investigated in Fig. 2. The characterization systems were schematically illustrated in Fig. S1. TENG was attached on a flat panel and followed excited by an oscillator. A force sensor was installed near the probe of the oscillator to record the loading force (presented in Fig. 2c). Keeping the frequency at 4 Hz, TENG with high sensitivity responds to the pressure of 0.3 N with voltage of 4.46 V, indicating it even enables to harvest weak mechanical energy (Fig. 2a). When the forces vary from 2 to 46 N, voltages of the TENG increase proportionally. Especially, the voltage tends to saturate when the force is larger than 32 N. The larger deformation of SST/PDMS induced by higher loading pressures leads to higher effective contacting areas and charges transformation at the interface. When the deformation of TENG reaches maximum, the full contact of TENG will lead to a saturated output voltage. Similarly, the output current presents the same tendency as it enhances from 0.04 to 0.80 μA under various forces (Fig. 2b). The electrical signals including voltage, current and the applied force also show ideal stability under 32 N (Fig. 2d–f). Additionally, the frequency-dependent electric outputs under 32 N are shown in Fig. 2g–i. Since higher loading frequency can decrease the duration of current peak and increase the charge-transfer process, [36,37] the voltage, current and output power undoubtedly elevate with the increasing of external loading frequencies (Fig. 2g, i) and the signals are also stable (Fig. 2h). The maximum voltage and current are respective 90.95 V and 0.91 μA at 10 Hz. Therefore, the optimized electrical performance of SST/PDMS-based TENG can be obtained under 32 N and 10 Hz.

The dependence of triboelectric properties of SST/PDMS-based TENG including voltage, current and output power on external load resistance were systematically studied. Voltage exhibits an increasing tendency (ranging from 8.61 to 112.79 V) with the elevation of external loading resistance (Fig. 3c). However, the currents show a reversely proportional relationship. The maximum current in the range of 1 MΩ–1 GΩ is 8.61 μA. The output power (P = UI) is calculated in Fig. 3d. The maximum peak power reaches 221.87 μW with the voltage of 42.13 V and current of 5.27 μA under the load resistance of 8 MΩ. Voltage and current show stability under 32 N and 10 Hz with 8 MΩ (Fig. 3a, b). These properties demonstrate SST/PDMS-based TENG is capable of collecting mechanical energy as a power source.

### *3.2. High-frequency energy-harvesting performance of SST/PDMS/PTFE-based TENG*

To improve the triboelectric output performance of TENG, various strategies have been taken out [38,39]. In this work, PTFE was introduced as an electrode component owing to its highest electron capturing characteristic and the influences of PTFE contents on the electrical properties of SST/PDMS/PTFE-based TENG were further explored. The tested samples were 5 × 5 $cm^2$ and the thickness kept at 2 mm. As expected, the maximum current of SST/PDMS/PTFE-1%-based TENG is 9.78 μA and it decreases with the increase of external resistance, while voltage simultaneously follows the opposite tendency (Fig. 4a). The maximum voltage is as high as 114.33 V. As depicted in

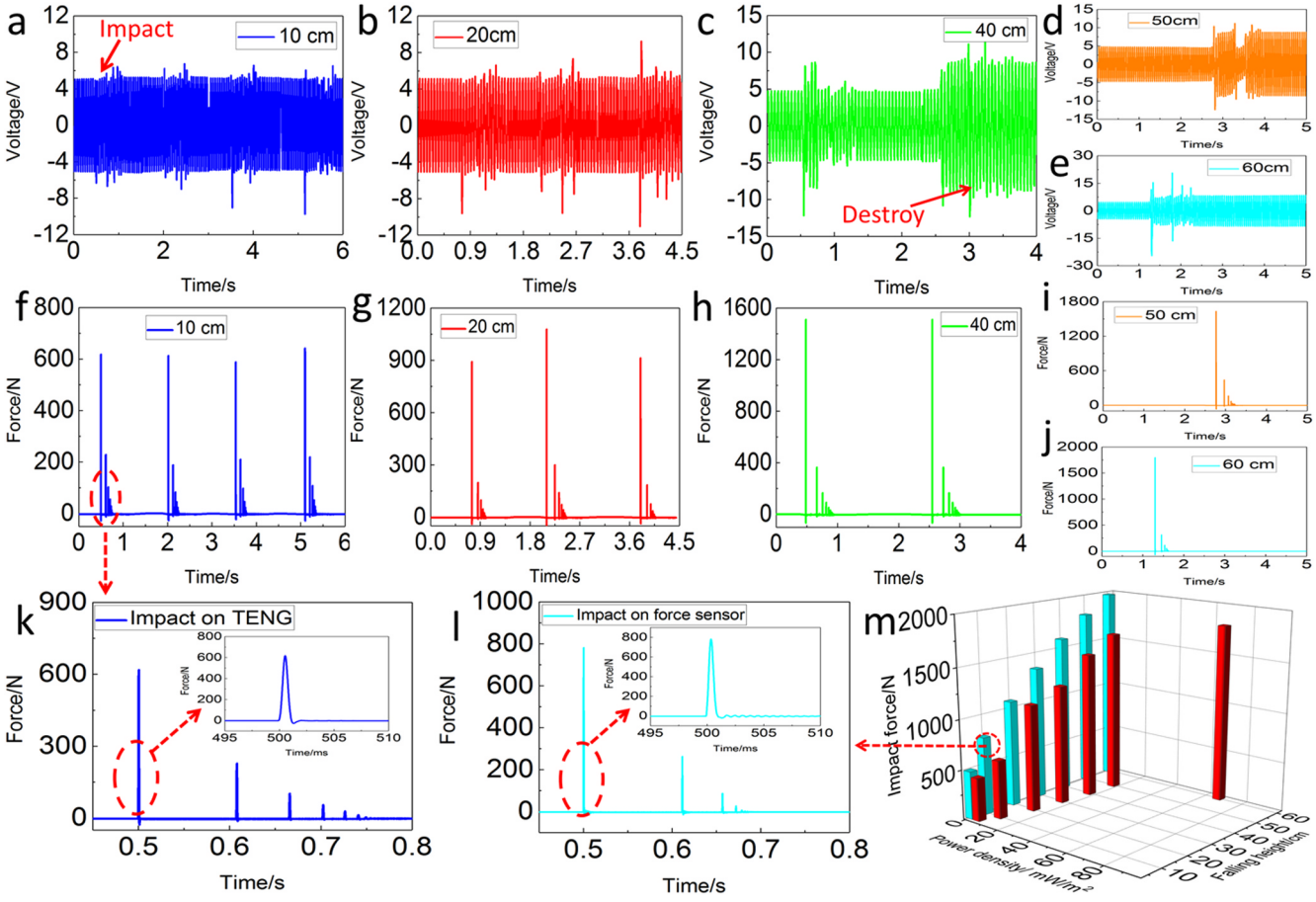


**Fig. 6.** Triboelectric and protection performance of TENG (2 mm) in low velocity impact tests: voltage and the corresponding force signals simulated by the impactor falling from (a, f) 10, (b, g) 20, (c, h) 40, (d, i) 50 and (e, j) 60 cm, respectively (the external resistance is 10 MΩ); typical force–time curves dropping on (k) TENG and (l) force sensor; (m) impact force and power density versus falling height in the 3D bar graph (red bars indicate the drop weight impact on TENG, blue bars represent the weight load on force transducer).

Fig. 4b, when the resistance is 8 MΩ, TENG reaches a voltage and current of 58.98 V and 7.37 μA (Fig. S2 a and b), and the maximum output power is 434.68 μW which shows 95.92% increment than the maximum power in Fig. 3d. This is due to the high capacity for harvesting electrons of PTFE [40]. Fig. 4c and d present the device enables to transfer the energy of human motion into electric energy which lights up more than 80 LEDs. Dependence of energy-harvesting performance of SST/PDMS/PTFE-3%-based TENG and SST/PDMS/PTFE-5%-based TENG on different external loading resistances are presented in Fig. 4h–k. Voltage and current show similar tendencies when compared with the results in Fig. 4a. The maximum electric power of SST/PDMS/PTFE-3%-based TENG achieves 395.40 μW at 7 MΩ and the corresponding voltage and current are presented in Fig. S2c, d. As for SST/PDMS/PTFE-5%-based TENG, the maximum power is 266.32 μW as the resistance is 10 MΩ (the relative voltage and current are shown in Fig. S2e, f). In this regard, SST/PDMS/PTFE-1%-based TENG exhibits the highest energy harvesting properties. When introduced PTFE, its highest ability of gathering electrons is favorable to improve the triboelectric output performance [41]. However, more PTFE nano-particles as well as their agglomerates expose on the surface of SST/PDMS with the increase of PTFE contents (Fig. 4e–g), they decrease the adhesion force between Al foil and SST/PDMS owing to its poor adhesion with other materials [42] which leads to a decreased contact area and lower triboelectric charges. On this occasion, the electrical properties decrease when PTFE contents increase from 3% to 5%. In conclusion, SST/PDMS/PTFE-1%-based TENG exhibits the highest energy harvesting property which is chosen for further study.

The properties of SST/PDMS/PTFE-1%-based TENG with various thicknesses are also explored since it plays important role in determining the ability of harvesting mechanical energy and the results are presented in Fig. 5. The instantaneous power of SST/PDMS/PTFE-1%-based TENG (4 mm) is maximized to 399.03 μW at an external resistance of 8 MΩ (voltage at 56.50 V and current at 7.06 μA, Fig. S3a, b). Additionally, an instantaneous output power of TENG with 6 mm achieves 44.20 V (Fig. S3c, d) and a peak value of 390.73 μW when the load resistance is about 5 MΩ (Fig. 5d). The slight decrease in maximum power density from 2 mm to 6 mm may due to the reduction of induced charges with the increase of thickness. Thicker polymer matrix with higher dielectric constant could prevent the charge accumulation which leads to lower output performance [25,43,44]. Additionally, thicker SST/PDMS/PTFE lay enables to absorb, store more kinetic energy and the collected energy for TENG is apparently decreased [45]. Thus, the triboelectric properties with thicker dielectric SST/PDMS/PTFE are decreased. As a sustainable power source, TENG (6 mm) is connected with a circuit composed of rectifier, different capacitors and LED array and the equivalent circuit is presented in Fig. 5e. The charging voltages as a function of charging time with different capacitances are shown in Fig. 5f. The voltage with smaller capacitance increases faster and 0.22 μF capacitor exhibits the highest voltage of 17.17 V within 45 s which verifies the high efficiency of harvesting high-frequency mechanical energy of TENG. Additionally, over 80 LED bulbs in series are lit up by the 0.22 μF capacitor (Fig. 5g). Durability test is further carried out by high-frequency loading-unloading on TENG for 4000 cycles since cyclic stability is important for practical application. According to Fig. 5h and i, SST/PDMS/PTFE-1%-based TENGs with 4 and 6 mm all exhibit excellent stability which the voltage signals show no degradation even

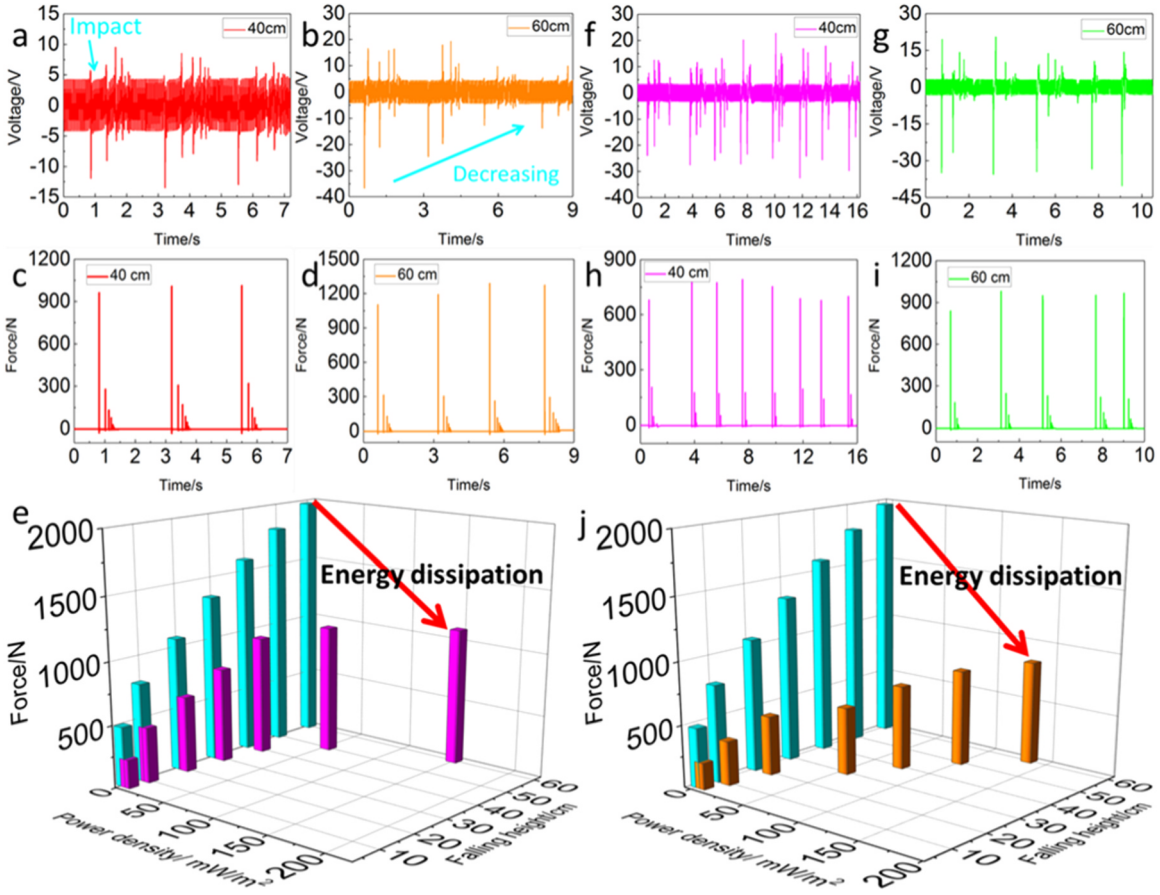


**Fig. 7.** Thickness dependent triboelectric and safeguarding performance of TENG under impact condition: voltage and the corresponding force signals simulated by the impactor falling from 40 cm on TENG with (a, c) 4 mm, (f, h) 6 mm, dropping from 60 cm on TENG with (b, d) 4 mm and (g, i) 6 mm, respectively; impact force and power density versus falling height in the 3D bar graph (red and yellow bars indicate the drop weight impact on TENG, blue bars represent the weight load on force transducer, the X-, Y- and Z-axis represent falling height, power density and force): TNEG with (e) 4 and (j) 6 mm.

after 4000 excitations. This result demonstrates SST/PDMS/PTFE-1%-based TENG with high electrical performance is appropriate as a self-powering energy source to actuate low-power electronic devices.

### *3.3. Safeguarding and low velocity impact energy collecting properties of TENG*

To further mimic the safeguarding as well as the low velocity energy harvesting properties of TENG, a drop hammer test system connecting with force sensor and digital multi-meter was employed to load-unload the impact excitation (Fig. S4). The head of the applied impactor is 3 × 3 cm. The impact force could be altered by changing the falling heights of the impactor. TENG was fixed on the metal force sensor which could record and transfer impact force after collision. The digital multi-meter could capture triboelectric signals. Once the impactor loads on TENG with the thickness of 2 mm, the force starts to increase to maximum 617.61 N within 0.70 ms and attenuate to 0 (Fig. 6f and k). The impactor then rebounds owing to the storage elastic energy of SST/PDMS/PTFE-1%. Fig. 6l is the force-time curves which the impactor are directly collided on force sensor. Compared with the peak value in Fig. 6l, the maximum force in Fig. 6k is significantly decreased by 21.05% (from 782.25 to 617.61 N) which proves TENG can act as a protector layer to absorb impact energy. When B atoms are introduced into polydimethylsiloxane chain, three Si-O-B polymer chains form [13]. The empty p orbits of B atoms would accept electrons from O atoms to form B-O dynamic cross bonds which are similar to the hydrogen bonds. Large numbers of the B-O cross bonds could attract neighboring polymer chains and impede their slide movement under high rate excitation. Simultaneously, the entangled polymer chains also obstruct the deformation and dissipate impact energy. Thus, shear stiffening effect occurs and the TENG device is able to dissipate energy. On the other hand, the impact forces as well as voltage increase with the increasing of falling heights which exhibits typical triboelectric characters. When the heights are 10 and 20 cm, the impact forces are 617.61 (Figs. 6f) and 890.73 N (Fig. 6g), respectively. The corresponding voltage are 6.70 (Figs. 6a) and 9.46 V (Fig. 6b). Voltage peaks are apparently in accordance with the changes of loading forces which implies the high response and sensitivity of TENG. Additionally, these stable signals demonstrate TENG can sustain the collisions effectively. Once the falling height is higher than 40 cm, TENG are easily destroyed according to the dramatic changes of voltage noise values (Fig. 6c–e). In addition, Fig. 6m is the results of maximum impact force and power density versus falling heights. Remarkably, power density of TENG shows characteristic enhancement from 4.61 to 67.24 μW/m$^2$ when the heights change from 5 cm to 60 cm. The impact force simultaneously exhibits similar increasing tendency. Compared with the forces loaded on force sensor (blue bar), the forces on TENG are relatively lower, indicating their energy-dissipating property. To this end, TENG shows triboelectric and protection performance under impact condition which illustrates the as-prepared TENG can harvest low-frequency impact kinetic energy as well as the favorable electrical and safeguarding stability during cycles of impact.

TENGs with different thicknesses were also investigated due to their significant influence on the properties of TENG. When the falling height is 40 cm, the stable voltage and force signals on TNEG (4 mm) prove SST/PDMS/PTFE-1% can effectively sustain the impact (Fig. 7a and c).

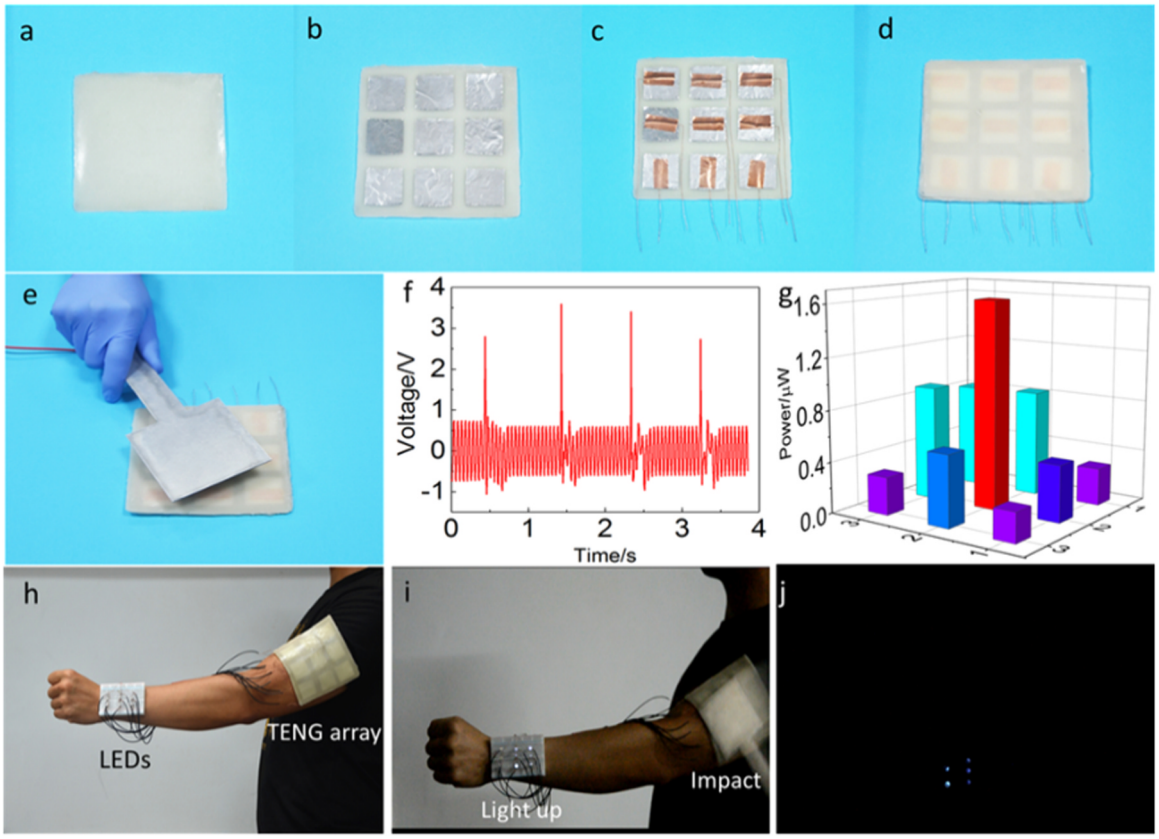


**Fig. 8.** Preparation procedures of (a–d) TENG arrays, typical (f) voltage-time signals and (g) the power distribution of TENG arrays excited (e) by impact, (h–j) TENG array acts as wearable power source to light up LEDs and protect human beings.

Keeping the falling height at 40 cm, TENG (4 mm) outputs stable voltages within 3 cyclic impact loadings which is owing to the triboelectrification and electrostatic induction (Fig. S5) The maximum voltage of TNEG (4 mm) attenuate from 36.75 to 12.69 V during cycles of impact when the falling height reaches 60 cm, indicating the structure of TENG (4 mm) is ruined (Fig. 7b, d). As for TENG (6 mm), voltage and impact forces keep stable in the falling heights of 5–60 cm, exhibiting better anti-impact performance (Fig. 7f–i, Fig. S6). The falling heights dependence of impact force and instantaneous power density of TENG with 4 and 6 mm are presented in Fig. 7e and j, respectively. The maximum force on force sensor is 1971.90 N (blue bar in Fig. 7j) at the dropping of 60 cm. However, they decrease to 1104.40 and 839.72 N for TENG (4 mm) and TENG (6 mm), respectively. The maximum power density for TENG (4 mm) is 150.06 μW/m$^2$ (Fig. 7e) while they elevate from 4.59 to 135.57 μW/m$^2$ when the falling heights vary from 5 to 60 cm (Fig. 7j). The favorable safeguarding and triboelectric stability of TENG-6 mm during cycles of harsh impact guarantee its good reliability for harvesting low velocity energy and safeguards. Additionally, TENG (6 mm) can scavenge impact energy generated by a hammer with the head of 5 × 5 cm$^2$ and lights up LEDs which shows potential application in powering small electronics (Movie S1).

Supplementary material related to this article can be found online at doi:10.1016/j.nanoen.2019.02.060.

### 3.4. TENG-based e-skin arrays

Finally, a SST/PDMS/PTFT-1%-based TENG (6 mm) array with 3 × 3 units and 12 × 12 cm$^2$ spatial resolution was obtained by sealing 9 pieces of Al foils (2.7 × 2.7 cm$^2$), conductive wires with polymer matrixes (Fig. 8a–d). The voltage signals were recorded during impact tests (Fig. 8e). Typically, voltage peaks are stable under cycles of impacts (Fig. 8f) and the output powers of all pieces are presented in Fig. 8g. The power distributions are in accordance with the loading forces distributions which the center of the single TENG exhibits the highest power of 3.60 μW. The TENG arrays can act as a wearable mechanoreceptor with energy-collecting properties which enables to light up the corresponding LEDs (Fig. 8h–j and Movie S2). Additionally, as a prototype of safeguard, the TENG array impedes external impact and protects human beings effectively.

Supplementary material related to this article can be found online at doi:10.1016/j.nanoen.2019.02.060.

## 4. Conclusion

In this paper, we reported a functional TENG with safeguarding property by resembling Al foil with SST/PDMS/PTFE polymer. The triboelectric property of TENG and the influence of PTFE contents and polymer thickness are systematically investigated. SST/PDMS/PTFE-1%-based TENG with the thickness of 6 mm shows a maximum power of 390.73 μW at voltage of 44.20 V. More importantly, it outputs an instantaneous power density of 135.57 μW/m$^2$ under impact as well as dissipates the force from 1971.90 to 839.72 N which presents its outstanding collecting and dissipating low velocity impact energy. Finally, a flexible TENG array can be used in wearable electronics and safeguards.

## Acknowledgement

Financial supports from the National Natural Science Foundation of China (Grant No. 11802303, 11772320), the Strategic Priority Research Program of the Chinese Academy of Sciences (Grant No. XDB22040502), the Fundamental Research Funds for the Central Universities (Grant No. WK2090050045), and China Postdoctoral Science Foundation (Grant No. 2018M632543) are gratefully

acknowledged. This study was also supported by the Collaborative Innovation Center of Suzhou Nano Science and Technology and partially carried out at the USTC Center for Micro and Nanoscale Research and Fabrication.

## Appendix A. Supporting information

Supplementary data associated with this article can be found in the online version at doi:10.1016/j.nanoen.2019.02.060.

## References

[1] A.M. Molan, A.A. Kordani, J. Transp. Eng. 140 (2014) (04014035-04014047).
[2] E. Khorshid, F. Alkalby, H.A. Kamal, J. Sound Vib. 304 (2007) 640–659.
[3] L.B. Tao, H. Song, S. Chakrabarti, J. Eng. Math. 65 (2009) 257–271.
[4] J.L. Cheng, H. Xu, Int. J. Solids. Struct. 43 (2006) 5355–5369.
[5] C.S. Boland, U. Khan, M. Binions, S. Barwich, J.B. Boland, D. Weaire, J.N. Coleman, Nanoscale 10 (2018) 5366–5375.
[6] K.H. Lam, Z.H. Chen, Y.Q. Ni, H.L.W. Chan, Sens. Actuators A: Phys. 158 (2010) 51–59.
[7] R.M. Millian, T. Ito, J.A. Loya, A. Olmedo, M.H. Miguelez, Mater. Des. 110 (2016) 391–403.
[8] J.W. Song, C.J. Chen, S.Z. Zhu, M.W. Zhu, J.Q. Dai, U. Ray, Y.J. Li, Y.D. Kuang, Y.F. Li, N. Quispe, Y.G. Yao, A. Gong, U.H. Leiste, H.A. Bruck, J.Y. Zhu, A. Vellore, H. Li, M.L. Minus, Z. Jia, A. Martini, T. Li, L.B. Hu, Nature 554 (2018) 224–228.
[9] S.R. Waitukaitis, H.M. Jaeger, Nature 487 (2012) 205–209.
[10] S. Wang, S.H. Xuan, Y.P. Wang, C.H. Xu, Y. Mao, M. Liu, L.F. Bai, W.Q. Jiang, X.L. Gong, ACS Appl. Mater. Interfaces. 8 (7) (2016) 4946–4954.
[11] Y.P. Wang, S. Wang, C.H. Xu, S.H. Xuan, W.Q. Jiang, X.L. Gong, Compos. Sci. Technol. 127 (2016) 169–176.
[12] S. Wang, S.H. Xuan, W.Q. Jiang, W.F. Jiang, L.X. Yan, Y. Mao, M. Liu, X.L. Gong, J. Mater. Chem. A 3 (2015) 19790–19799.
[13] S. Wang, W.Q. Jiang, W.F. Jiang, F. Ye, Y. Mao, S.H. Xuan, X.L. Gong, J. Mater. Chem. C 2 (2014) 7133–7140.
[14] C.H. Xu, Y. Wang, J. Wu, S.C. Song, S.S. Cao, S.H. Xuan, W.Q. Jiang, X.L. Gong, Compos. Sci. Technol. 153 (2017) 168–177.
[15] F.R. Fan, Z.Q. Tian, Z.L. Wang, Nano Energy 1 (2012) 328–334.
[16] A. Proto, M. Penhaker, S. Conforto, M. Schmid, Trends Biotechnol. 35 (2017) 610–624.
[17] D. Bhatia, W. Kim, S. Lee, S.W. Kim, D. Choi, Nano Energy 33 (2017) 515–521.
[18] R.Y. Liu, X. Kuang, J.N. Deng, Y.C. Wang, A.C. Wang, W.B. Ding, Y.C. Lai, J. Chen, P.H. Wang, Z.Q. Lin, J.H. Qi, B.Q. Sun, Z.L. Wang, Adv. Mater. 30 (2018) 1705195–1705203.
[19] S.Y. Gao, J.Z. Su, M. Wang, X.J. Wei, X. Zheng, T. Jiang, Nano Energy 30 (2016) 52–58.
[20] X. Zheng, J.Z. Su, X.J. Wei, T. Jiang, S.Y. Gao, Z.L. Wang, Adv. Mater. 28 (2016) 5188–5194.
[21] L. Lin, S.H. Wang, Y.N. Xie, Q.S. Jing, S.M. Niu, Y.F. Hu, Z.L. Wang, Nano Lett. 13 (2013) 2916–2923.
[22] H.L. Zhang, Y. Yang, X.D. Zhong, Y.J. Su, Y.S. Zhou, C.G. Hu, Z.L. Wang, ACS Nano 8 (2014) 680–689.
[23] S.W. Chen, X. Cao, N. Wang, L. Ma, H.R. Zhu, M. Willander, Y. Jie, Z.L. Wang, Adv. Energy Mater. 7 (2017) 1601255–1601264.
[24] Y.J. Su, G.Z. Xie, F.B. Xie, T. Xie, Q.P. Zhang, H.L. Zhang, H.F. Du, X.S. Du, Y.D. Jiang, Chem. Phys. Lett. 653 (2016) 96–100.
[25] Y. Xi, J. Wang, Y.L. Zi, X.G. Li, C.B. Han, X. Cao, C.G. Hu, Z.L. Wang, Nano Energy 38 (2017) 101–108.
[26] Y. Chen, M. Wang, M. Tian, Y.Z. Zhu, X.J. Wei, T. Jiang, S.Y. Gao, Nano Energy 42 (2017) 314–321.
[27] S.Y. Gao, M. Wang, Y. Chen, M. Tian, Y.Z. Zhu, X.J. Wei, T. Jiang, Nano Energy 45 (2018) 21–27.
[28] J.M. Ma, T. Zhou, J. Bian, Y. Jie, X. Cao, N. Wang, Nano Energy 44 (2018) 199–207.
[29] H. Xue, Q. Yang, D.Y. Wang, W.J. Luo, W.Q. Wang, M.S. Lin, D.L. Liang, Q.M. Luo, Nano Energy 38 (2017) 147–154.
[30] S.B. Jeon, Y.H. Nho, S.J. Park, W.G. Kim, I.W. Tcho, D. Kim, D.S. Kwon, Y.K. Choi, Nano Energy 41 (2017) 139–147.
[31] H.J. Guo, T. Li, X.T. Cao, J. Xiong, Y. Jie, M. Willander, X. Cao, N. Wang, Z.L. Wang, ACS Nano 11 (2017) 856–864.
[32] K.R. Dai, X.F. Wang, F. Yi, C. Jiang, R. Li, Z. You, Nano Energy 45 (2018) 84–93.
[33] J. Chen, Y. Huang, N.N. Zhang, H.Y. Zou, R.Y. Liu, C.Y. Tao, X. Fan, Z.L. Wang, Nat. Energy 1 (2016) 16238–16246.
[34] J.Q. Xiong, M.F. Lin, J.X. Wang, S.L. Gaw, K. Parida, P.S. Lee, Adv. Energy Mater. 7 (2017) 1701243–1701253.
[35] J.W. Zhong, Q.Z. Zhong, G.J. Chen, B. Hu, S. Zhao, X. Li, N. Wu, W.B. Li, H.M. Yu, J. Zhou, Eng. Environ. Sci. 9 (2016) 3085–3091.
[36] Z.L. Li, J.L. Shen, L. Abdalla, J.Y. Yu, B. Ding, Nano Energy 36 (2017) 341–348.
[37] P.K. Yang, L. Lin, F. Yi, X.H. Li, K.C. Pradel, Y.L. Zi, C.I. Wu, J.H. He, Y. Zhang, Z.L. Wang, Adv. Mater. 27 (2015) 3817–3824.
[38] B. Chen, Y. Yang, Z.L. Wang, Adv. Energy Mater. 8 (2018) 1702649–1702662.
[39] M.M.A. Parvez, H. Nazmul, F.S. Hisan, A. Mohsen, L. Candace, Adv. Energy Mater. 8 (2018) 1701210–1701235.
[40] M. Wang, N. Zhang, Y.J. Tang, H. Zhang, C. Ning, L. Tian, W.H. Li, J.H. Zhang, Y.C. Mao, E.J. Liang, J. Mater. Chem. A 5 (2017) 12252–12257.
[41] H.Y. Li, L. Su, S.Y. Kuang, Y.J. Fan, Y. Wu, Z.L. Wang, G. Zhu, Nano Res. 10 (2017) 785–793.
[42] R.I. Haque, P.A. Farine, D. Briand, Sens. Actuators A Phys. 271 (2018) 88–95.
[43] X. Wang, Y. Yin, F. Yi, K. Dai, S. Niu, Y. Han, Y. Zhang, Z. You, Nano Energy 39 (2017) 429–436.
[44] P. Kaushik, K. Vipin, J.X. Wang, B. Venkateswarlu, B. Ramaraju, S.L. Pooi, Adv. Mater. 29 (2017) 1702181–1702189.
[45] H.Y. Qiao, Y. Zhang, Z.G. Huang, Y.M. Wang, D.Q. Li, H.M. Zhou, Nano Energy 50 (2018) 126–132.

**Dr. Sheng Wang** received his Ph.D. degree from University of Science and Technology of China in 2017. Now he is a postdoctoral fellow in the Chinese Academy of Sciences Key Laboratory of Mechanical Behavior and Design of Materials in Hefei, China. His research interests include smart materials and devices with magnetic, electric and force-sensing properties. He is also currently interested in developing multifunctional triboelectric nanogenerator systems.

**Li Ding** received her B.S. degree in Astronautic Engineering and Mechanics from Harbin Institute of Technology, Harbin, Heilongjiang, PR China in 2015. She is currently a Ph.D. candidate in Department of Modern Mechanics at University of Science and Technology of China. Her research interests are focused on smart sensing materials and magnetically controllable devices.

**Yu Wang** is an Associate Professor in the Department of Modern Mechanics, University of Science and Technology of China (USTC). He received his B.Sc. and Ph.D. from the USTC. After graduation, he also worked as a visiting scholar in Hong Kong University of Science and Technology for 1 year. Dr. Wang's research interests include on the mechanical behaviors and its constitutive characterization of soft materials with the multi-physics coupling properties for sensing and safeguard application.

**Dr. Xinglong Gong** received his Ph.D. degree in Mechanics from both the University of Science and Technology of China (USTC, China) and Saitama University (Japan), in 1996. Then, he worked at the Nihon Dempa Kogyo Co., Ltd., Japan. In 2003, he joined the Department of Modern Mechanics, USTC, as a Full Professor. He is currently the council chairman of Chinese Society of Experimental Mechanics. His research interests comprise soft matter materials as well as their applications. He was supported by the 100-Talent Programme of Chinese Academy of Sciences in 2003 and supported by the National Science Foundation for Distinguished Young Scholars of China in 2011.